J. Webster (ed.), *Wiley Encyclopedia of Electrical and Electronics Engineering*


# COGENERATION

Cogeneration is the simultaneous generation of mechanical/electric and thermal power. Cogeneration is not a new technology and has long been recognized as one of the most technically sound means of improving the thermodynamic energy conversion process. It is a practice that has been widely used in many industrial plants as an economical means of providing a portion or all of the plant's electric–mechanical power needs and generating its process heating requirements as a by-product of the power requirements or vice versa. Successful applications in the chemical, petroleum refining, metals and mining, pulp and paper, and food industries, as well as in industries with smaller heat loads, such as university complexes and hospitals, attest to the wide acceptability of cogeneration as a reliable, economical way of providing different forms of useful energy. Increased interest in cogeneration is demonstrated by the wide variety of prime movers and plant arrangements (1) now being proposed in a field that has always been dominated by steam cycles and internal combustion engines.

In the following the main aspects of the cogeneration system will be presented and discussed.

## Overall Analysis

Cogeneration systems can be based on two different layouts: topping or bottoming arrangements (Fig. 1). In the topping case the electric power is generated by the use of an engine operating at high temperature and the process heat is recovered from the waste heat from the engine [Fig. 1(a)]. Vice versa, in the bottoming arrangement [Fig. 1(b)] the engine's primary energy is the waste heat of the topping heat generation process (industrial process).

As shown in Fig. 2, the primary energy for a topping layout coincides with the fuel energy, and four different energy flows can be considered: power ($W$), useful heat ($Q_u$), lost heat ($Q_{lost}$), and primary energy fuel ($F$). The *first-law efficiency* of the system is the ratio between power and fuel ($W/F$), the *thermal efficiency* is equal to $Q_u/F$, and the *ratio of heat to power* is $W/Q_u$. These traditional performance criteria have limited relevance to a cogeneration system that provides heat and generates electric power. A more logical criterion is the *energy utilization factor* (*EUF*), used by Porter and Mastanaiah (2):

$$\mathrm{EUF} = \frac{W + Q_u}{F} \qquad (1)$$

It is preferable not to use the term efficiency for the EUF, to avoid confusion with the thermal or first-law efficiency ($\eta_I = W/F$).

However, as pointed out by Horlock (3), it must be remembered that the work $W$ is more difficult to produce and high-priced, whereas the useful heat $Q_u$ is usually a lower-grade, lower-priced product of the plant. The EUF is therefore not entirely satisfactory as a performance criterion, as it gives equal weight to work $W$ and

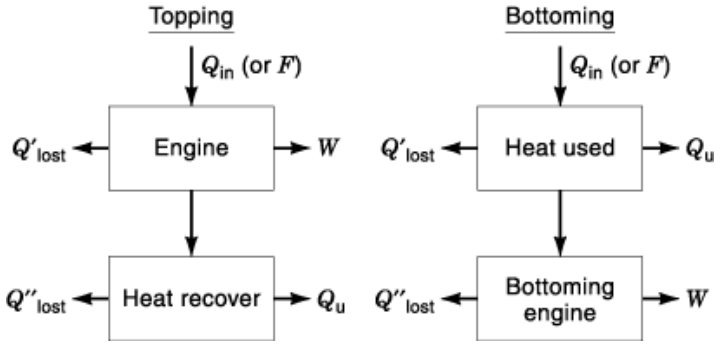


**Fig. 1.** Topping and bottoming heat recovery layouts.

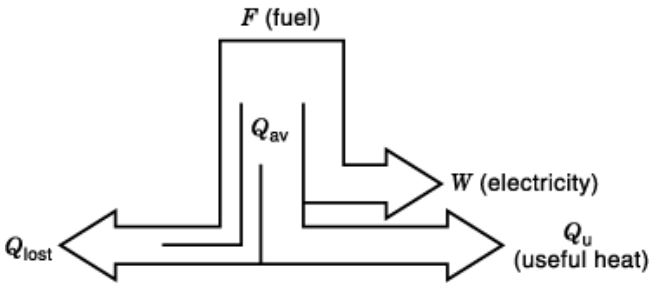


**Fig. 2.** Topping heat recovery layout.

heat $Q_u$. A first attempt to overcome this problem is the introduction of a *second-law efficiency* defined as

$$n_{II} = \frac{W + Q_u(1 - T_0/T_x)}{F} \tag{2}$$

where $T_0$ is the environment temperature, and $T_x$ the $Q_u$ temperature (or an average value of it). From the thermodynamic point of view Eq. (2) is obviously correct. However, with its use the value assigned to the useful heat is very low and the possible gain using a cogeneration system will not be evident.

An alternative performance criterion sometimes used is an *artificial thermal efficiency* $\eta_\alpha$, in which the energy in the fuel supply to the cogeneration plant is supposed to be reduced by that which would be required to produce the heat load in a separate heat-only boiler of efficiency $\eta_B$, i.e. $Q_u/\eta_B$. The artificial efficiency $\eta_\alpha$ is then given by

$$\eta_a = \frac{W}{F - (Q_u/\eta_B)} = \frac{\eta_{cog}}{1 - (Q_u/\eta_B F)} \tag{3}$$

where $\eta_{cog}$ is the overall efficiency of the cogeneration plant.

Another useful performance criterion involves the comparison of the fuel required to meet the given load for electricity and heat in the cogeneration plant with that required in separate conventional plants to meet the same loads (Fig. 3), say in a conventional electric power station of overall efficiency $\eta_e$ and a heat-only boiler

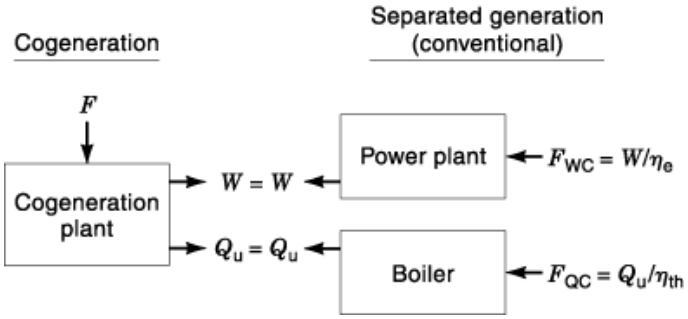


**Fig. 3.** Separated heat and power generation (conventional plant) and cogeneration system.

of efficiency $\eta_{th}$. Then the fuel energy saved is

$$\Delta F = F_{conv} - F_{cog} = \frac{Q_u}{\eta_{th}} + \frac{W}{\eta_e} - F_{cog} \tag{4}$$

and the *fuel energy savings ratio* (*FESR*) is defined as the ratio of the saving ($\Delta F$) to the fuel energy required in the conventional plants:

$$\begin{aligned} \text{FESR} &= \frac{F_{conv} - F_{cog}}{F_{conv}} = 1 - \frac{F_{cog}}{F_{conv}} \\ &= 1 - \frac{F_{cog}}{(Q_u/\eta_{th})(W/\eta_e)} \end{aligned} \tag{5}$$

This thermodynamic performance criterion is perhaps the most useful yet described, as it can be used directly in an economic assessment of a cogeneration plant.

The evaluation of the reference efficiencies $\eta_e$ and $\eta_{th}$ is necessary in order to use the FESR index. For the electrical efficiency it is possible to consider the average value of the existing electric power plants (utilities), or the efficiency of the "best plant" (combined plants), $\eta_e = 0.54$ to 0.58. The same can be done for the thermal efficiency; for conventional boilers, depending on the application and the size, it is 0.50 to 0.90.

A contour representation of the index is shown in Fig. 4; the thermal efficiency $\eta_{th}$ is plotted on the $x$ axis and the electrical efficiency $\eta_e$ on the $y$ axis. By varying the values of $\eta_{th}$ and $\eta_e$, different scenarios can be obtained. Figure 4(a) shows the case when $\eta_e = 35\%$ and $\eta_{th} = 75\%$; Fig. 4(b), $\eta_e = 37\%$ and $\eta_{th} = 80\%$; and Fig. 4(c), $\eta_e = 52\%$ and $\eta_{th} = 85\%$. Lines of equal FESR are shown (obviously only the bottom left triangle of the plot has a physical meaning).

The FESR in the first case can be very high, as the comparison is carried out with small-size, low-efficiency conventional plants (for civil application). The FESR value depends on the technological level of the cogeneration plant. In the second case [Fig. 4b] the FESR values are obviously lower for given $\eta_{th}$ and $\eta_e$. The case shown here is representative of a medium-size cogeneration plant for industrial application. The last case is representative of a very large-size industrial plant, and the comparison is carried out with the best available energy conversion technology (large natural-gas boiler and advanced combined plant). In this case the FESR index is reduced, and its maximum value is around 40% [versus > 60% in Fig. 4(a)].

To better understand the interest in the FESR values, Fig. 5 shows the performance of the most-used cogeneration systems on the same plot (they will be presented and discussed in detail in the next section). In

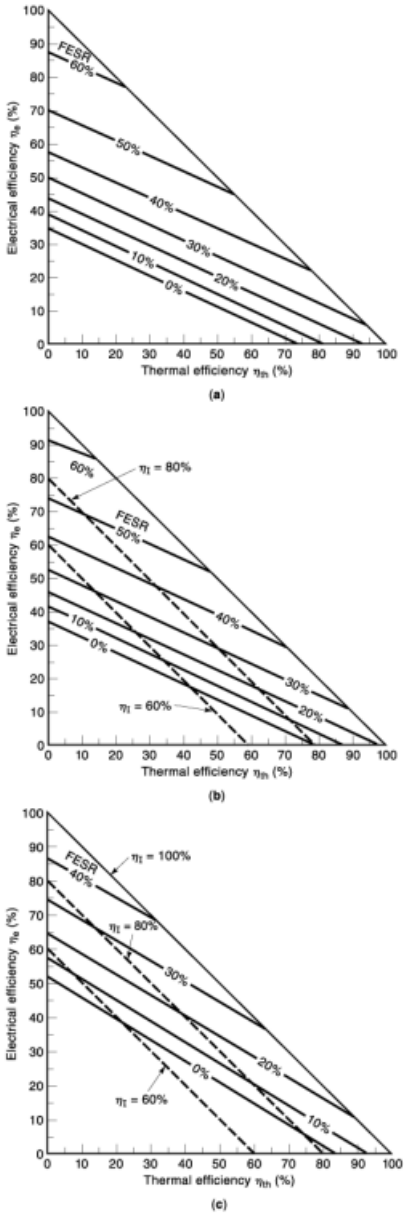


**Fig. 4.** Contours of fuel energy saving ratio for different $\eta_{th}$ and $\eta_e$: (a) $\eta_{th} = 0.50$, $\eta_e = 0.35$; (b) $\eta_{th} = 0.80$, $\eta_e = 0.37$; (c) $\eta_{th} = 0.85$, $\eta_e = 0.52$.

the figure the performance of the traditional boiler and of plants only generating electricity are also shown (the former on the $x$ axis, and the latter on the $y$ axis). The index is minimum for steam turbines and maximum for combined cycles. It is interesting to plot the lines at FESR =0 for the three previous cases shown in Fig. 4. For the first case ($\eta_e = 0.35$, $\eta_{th} = 0.75$) all the cogeneration systems allow a positive value of the FESR to be obtained; in the second case ($\eta_e = 0.37$, $\eta_{th} = 0.80$) internal combustion engines (*ICE*s) with partial recovery of

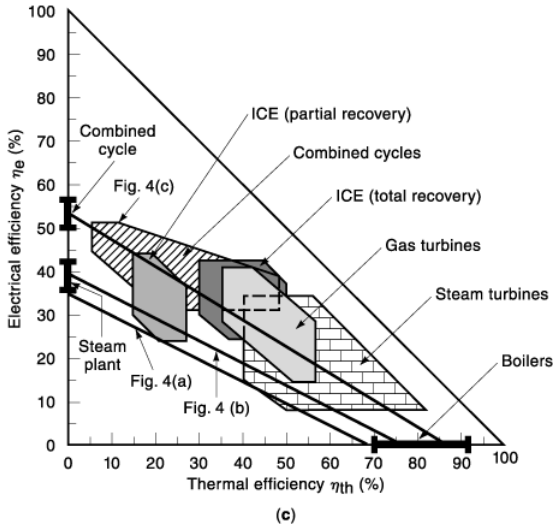


**Fig. 5.** Fuel energy saving ratio for several cogeneration layouts.

the waste heat and steam turbines do not allow the FESR to be positive; in the third case ($\eta_e = 0.52$; $\eta_{th} = 0.85$) only advanced solutions allow a positive value.

## Cogeneration Systems

Figure 6 presents seven alternative cogeneration plants considered in this presentation:

- Simple-cycle gas turbine (*GT*) engine with a heat recovery steam generator (*HRSG*) [Fig. 6(a)]: Gas-turbine-based cogeneration systems are characterized by rather low thermal/electric power ratios and by the ability to produce heat at relatively high temperatures.
- Back-pressure steam turbine (*BPST*) [Fig. 6(d)]: Back-pressure systems represent the simplest steam turbine plant arrangement and are widely used in low-power-output industrial applications. They are characterized by relatively poor thermodynamic performance and large heat-to-electricity ratios. Usually the power is controlled through a throttling valve at the turbine inlet. Variable-boiler-pressure control is not of interest, since it would not yield significant improvements in the combustion-gas heat recovery fraction. Since the first stage of steam turbines normally operates in choked conditions, the throttling valve acts by reducing both pressure and steam flow rate at the turbine inlet.
- ICE with unfired HRSG [Fig. 6(c)]: Such systems are commercially available in a wide range of power outputs, from small (10 kW to 50 kW) automobile-derived engines to large (over 10 MW) low-speed diesel or gas engines. They are highly efficient systems characterized by low heat-to-electricity ratios. While heat recovery from the exhaust gases always occurs, in low-temperature applications heat can also be recovered from other sources (engine coolant, oil, supercharger).
- Extraction–condensing steam turbine (ECST) [Fig. 6(e)]: This solution is widely used for large-power-output plants, and, compared to back-pressure systems, yields higher electric efficiencies and flexibility but with higher plant complexity. The steam conditions at the boiler exit are usually assumed to be constant, and the total steam flow rate is controlled by a throttling valve at the high-pressure turbine inlet. A second

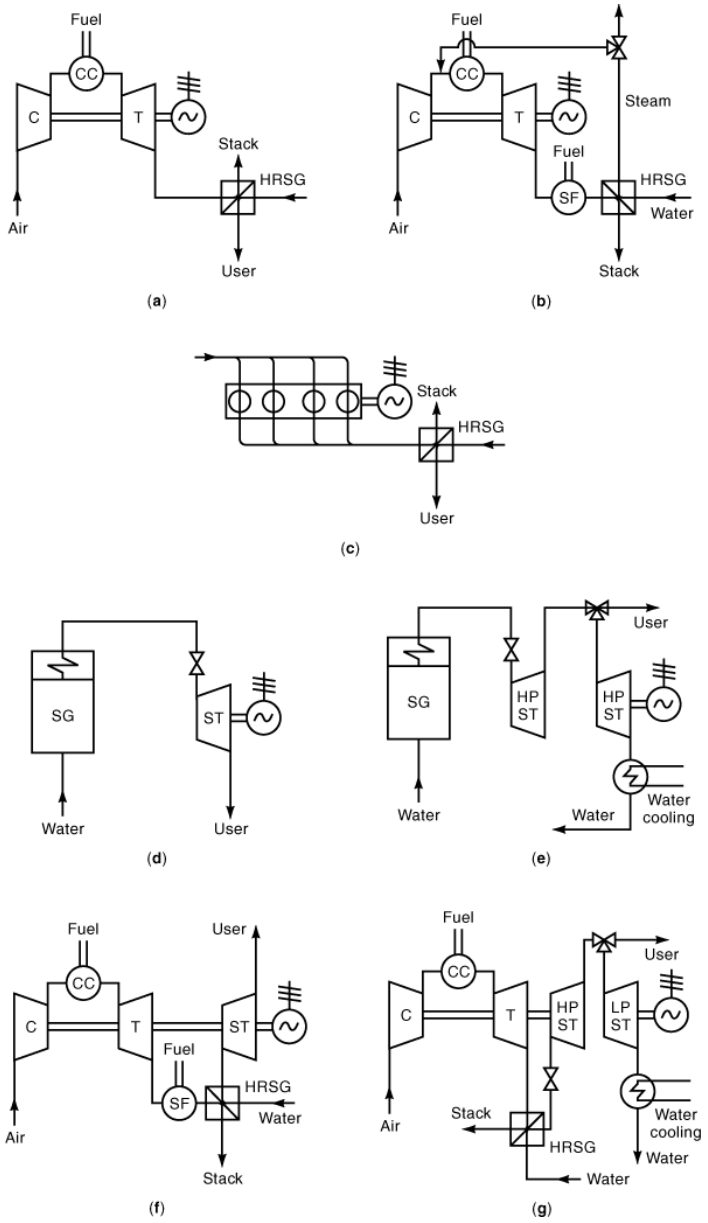


**Fig. 6.** Different cogeneration plant layouts: (a) gas turbine (GT); (b) steam-injected GT (STIG) with supplementary firing (SF); (c) internal combustion engine (ICE); (d) back-pressure steam turbine (BPST); (e) extraction–condensing steam turbine (ECST); (f) combined-cycle BPST; (g) combined-cycle ECST.

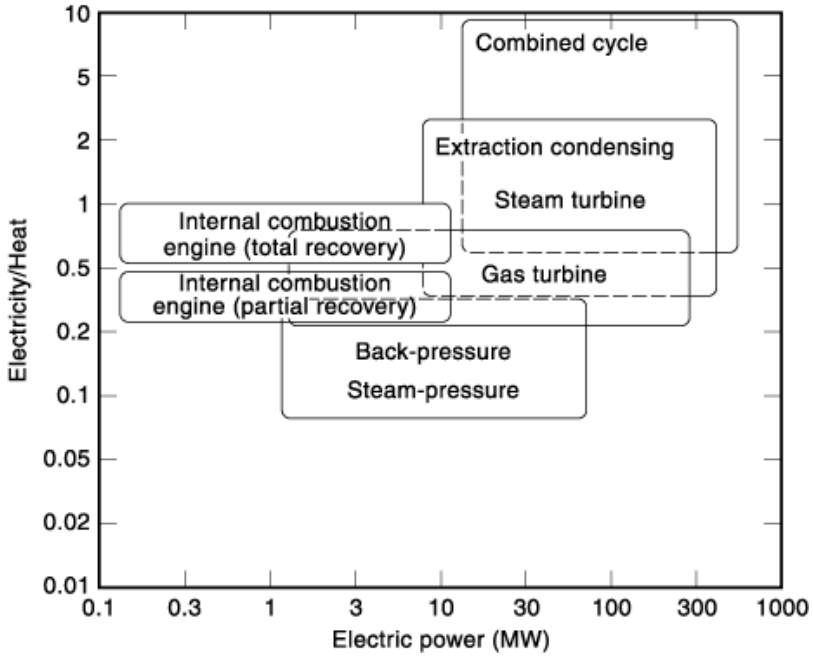


**Fig. 7.** Fields of application of the cogeneration systems shown in Fig. 6.

valve at the high-pressure turbine outlet controls the ratio between low-pressure and the high-pressure flow.

- Steam-injected gas turbine (*STIG*) with supplementary-fired (*SF*) HRSG [Fig. 6(b)]: Aside from their potential in power generation, STIGs are particularly attractive for cogeneration in that when thermal demand is low (or electrical energy is expenssive) the steam produced in the HRSG can be diverted to the gas turbine, thus increasing efficiency and electrical power output.
- Combined cycle (*CC*), comprising a gas turbine, a SF HRSG, and a steam cycle with a BPST [Fig. 6(f)].
- CC, comprising a gas turbine, a SF HRSG, and a steam cycle with an ECST [Fig. 6(g)].

CCs, when used for central stations, show net electrical efficiencies of over 55% for large installed systems (200 MW to 400 MW). They are used for large cogeneration systems (over 100 MW) for district heating. Depending on the size and specific application, the arrangement of the steam section may vary substantially: extraction–condensing cycles are economically justified only for large installations, while small systems generally consist of a simple back-pressure turbines.

Figure 7 summarizes the fields of application of the described cogeneration systems in terms of electricity-to-heat ratio in proportion to electric power (size of the plant). It is quite evident that for small plants ($<$1 MW) the ICE is the best choice, while in the range between 1 MW and 10 MW different solutions are possible depending on the electricity-to-heat ratio. For systems operating at higher electrical power ($>$10 MW) the choice is determined by the electricity-to-heat ratio.

Another interesting aspect useful for comparing the different cogeneration layouts is the efficiency. Figure 8 shows, as an example, a diagram where the electrical efficiency of the cogeneration plant is plotted against the electric power. The data are representative of medium-large cogeneration systems.

**Off-design performance.** As already discussed, one of the most important parameters for a cogeneration plant is the heat-to-electricity ratio. This value has been considered in the previous section only at the

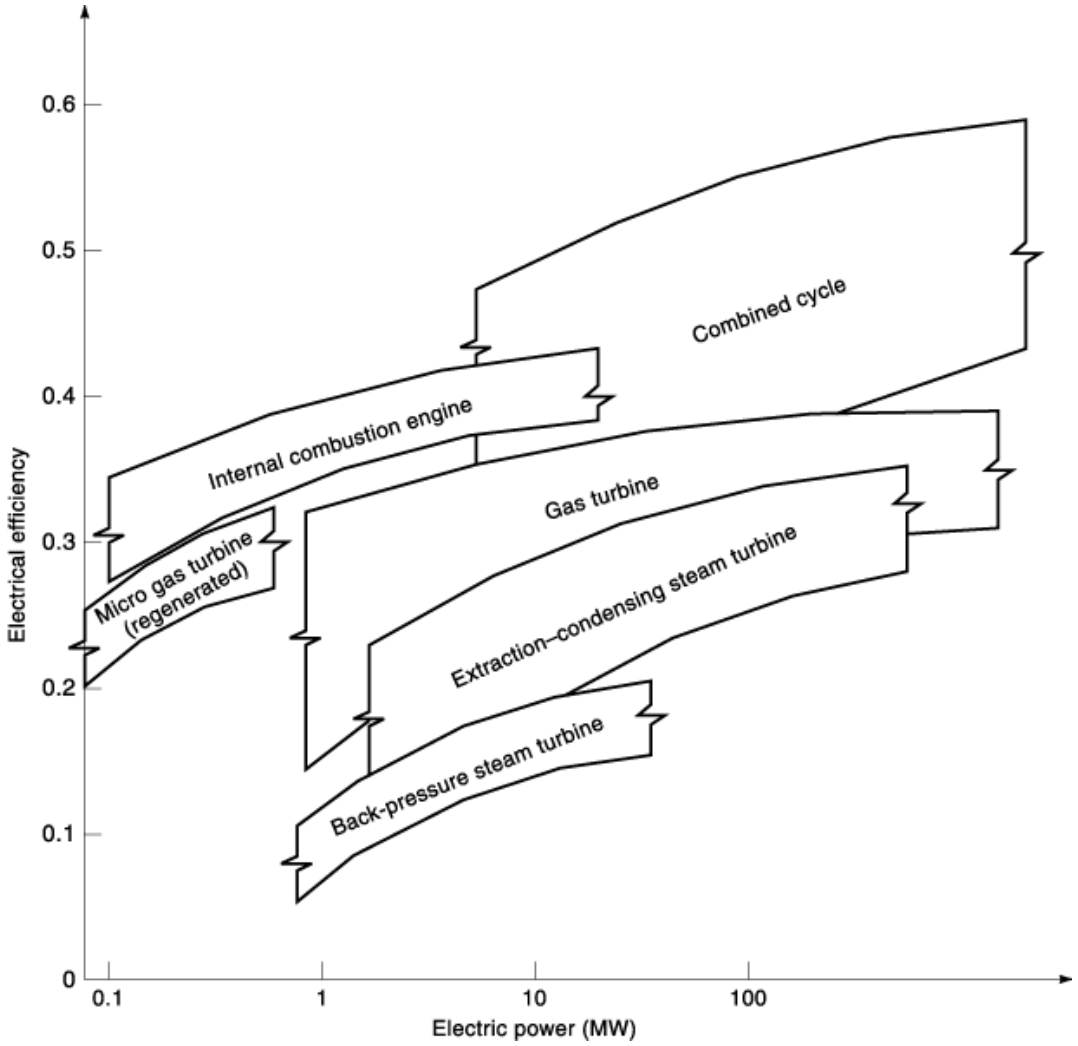


**Fig. 8.** Electrical efficiency versus electric power of several cogeneration layouts.

design point of the plant. Unfortunately, in a cogeneration application the electrical and thermal output of the prime mover are variables, the plant is generally connected to the grid, and there is always the possibility of the existence of an auxiliary boiler. In fact, a cogeneration plant is likely to experience a time-dependent pattern of electrical and thermal demand; hence, calculations based only on design or average operating conditions generally have limited value. Further complications can be introduced by the possibility of thermal storage, which makes the thermal load profile a subject of optimization rather than a specified input.

The cogeneration layout already presented can be divided into two categories: one degree of freedom, and two or more degrees of freedom, as shown in Fig. 9. Electric power and thermal power are shown for the performance of the two different types of plant in the plot. For a one-degree-of-freedom plant the modification of the electric power is strictly connected to the thermal-power change (the plant is represented only by a line in the diagram). In the case of a two-degree-of freedom plant, the possible combinations of thermal and electric power operating conditions are inside the gray region of the figure.

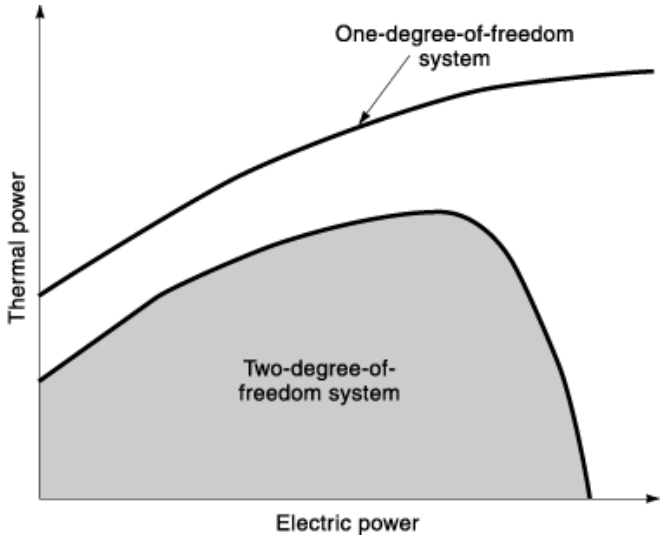


**Fig. 9.** Performance curves for one- and two-degree-of-freedom cogeneration plants.

One-degree-of-freedom plants are ICE, GT, BPST, and CC with BPST; two-degree-of-freedom plants are ECST, CC with ECST, and STIG.

Thanks to the possibility of diverting steam to the LP turbine in the ECST plant, one more degree of freedom, than in BPST is introduced and allows coverage of the whole operating region without dumping unused heat. Similar considerations can be carried out for CC ECST plants.

The STIG solution is very interesting from the point of view of degrees of freedom. The electric power can be varied independently. In fact, the generated steam can be used to generate more electric power (steam injection) or to produce useful heat.

A very interesting and useful comparison of the thermodynamic off-design performance of the cited cogeneration plants is reported by Consonni et al. (4).

The influence of supplementary firing is another important aspect of the cogeneration systems. Figure 10 shows, as an example, the operating field of a one-degree-of-freedom plant including supplementary firing. Point $A$ is the design point, and $B$ is the minimum-output point. Below the line $AB$ the excess heat must be dissipated. Above the line $AB$ (gray area) the effect of the supplementary firing is evident. The points $C$ and $D$ correspond to $A$ and $B$ but with the maximum value of supplementary firing. The points inside the gray area are representative of a heat-to-electricity ratio different from those on the line $AB$. The line $CD$ is associated with technological constraints (complete fuel combustion, gas temperature, emission control).

It is interesting to note that in such a situation the point $E$ in the figure has fixed electricity and heat values, but they can be obtained in different ways. At point $A$, the electricity is in excess, and it can be sold to the grid; also the thermal power is in excess, and part of the waste gas is sent to the bypass stack. At point $G$, the prime mover satisfies the thermal power requirement and the electricity is in excess. At point $F$, the electrical demand is satisfied, but supplementary firing is necessary to satisfy the thermal power requirement. At point $B$, the heat power requirement calls for the use of supplementary firing, while to satisfy the electrical demand it is necessary to buy electricity from the grid (working at point $B$ to avoid shutting down the plant).

Figure 11 shows the operating performance of a STIG with supplementary firing. In this case the choice of the most economical operating point is more complex, due to the degrees of freedom of the system. (gas turbine fuel control, steam injection control, supplementary firing). Also in this case the choice of the operating conditions must be based on the best economic performance of the cogeneration system.

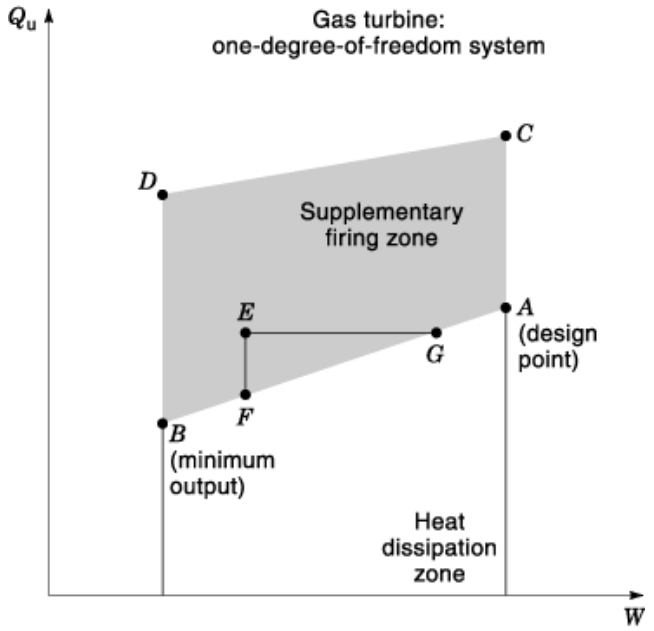


**Fig. 10.** Useful heat versus electricity for a one-degree-of-freedom cogeneration plant.

The line *AB* is the operating line without steam injection and supplementary firing; the line *BC* represents maximum electrical generation with steam injection. The gray area represents the operating conditions where supplementary firing is used. Obviously, a similar diagram can be presented for the other cogeneration plants reported in Fig. 6.

## Design of Cogeneration Systems

In addition to the difficulties encountered by utilities in specifying the design characteristics of central power plants, for a cogeneration plant the specifications are further complicated by the following issues:

- A choice must be made from a wide range of prime movers and plant arrangements.
- Since the cogeneration plant is usually connected to the grid and an auxiliary boiler should be present, the electrical and thermal design outputs of the prime mover are variables to be decided during the plant design phase.
- The electrical and thermal demands show a time-dependent pattern; hence calculations based on design or average operating conditions have limited value.
- A cogeneration plant generates two useful products, electricity and heat, having different thermodynamic values and also different economic values.

Figure 12 summarizes the main factors to be taken into account in the design of cogeneration plants. Economic or energy-saving properties are often used as evaluation criteria in the fundamental design of cogeneration plants, and they are influenced by the factors shown in Fig. 12. They are categorized into (A)

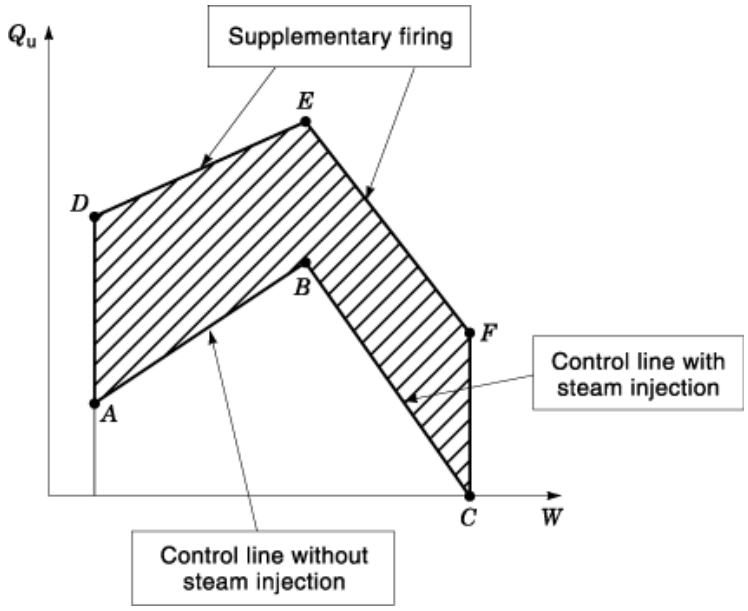


**Fig. 11.** Useful heat versus electricity for a two-degree-of-freedom cogeneration plant.

plant, (B) input energy, (C) output energy, (D) energy management, and (E) environment. These factors should be taken into account comprehensively.

At present, a trial-and-error method is conventionally used to determine plant size; viz., economic and energy properties are evaluated only for a few alternatives with regard to equipment capacity and maximum utility demands, from which the best alternative is selected. Additionally, the thermal and electrical *following strategies* are adopted conventionally as operational strategies for prime movers.

These conventional approaches have the disadvantage that the high economic and energy-saving potentials of cogeneration sometimes cannot be realized. Moreover, as a cogeneration system has always at least one degree of freedom, changing prices and changing thermal and electrical demand pose the question of what is the optimum operating point for each set of demands and prices. While for one-degree-of-freedom systems the answer may be found without resorting to sophisticated numerical techniques, for multi-degree-of-freedom systems the task is rather complex.

Although the subject of cogeneration system optimization has been addressed in quite a number of papers, the authors usually have referred to steady-state or design operation and/or neglected the variability of the prices of electricity and heat. Some authors have considered the influence of off-design performance and/or time-of-day electricity price variations: Consonni et al. (4) proposed an optimum approach for the strategy of a cogeneration plant, and Yokoyama et al. (5) proposed a complete optimum sizing and operational strategy. All the above approaches utilize linearized performance curves for the prime movers.

In the following, a method (6) similar to one proposed by the cited authors but without the linearization hypothesis (a complete nonlinear solution) will be presented as a useful approach for the optimum sizing and operational strategy for cogeneration plants. Figure 13 shows the hierarchical procedure utilized to determine the sizes and operational strategies of the plants. The basic concept is the minimization of the total annual cost from the long-term economic point of view. It is evaluated as the sum of the annual capital cost and annual running cost on the basis of an annualized cost method. The annual capital cost of each piece of equipment is considered as a function of its capacity.

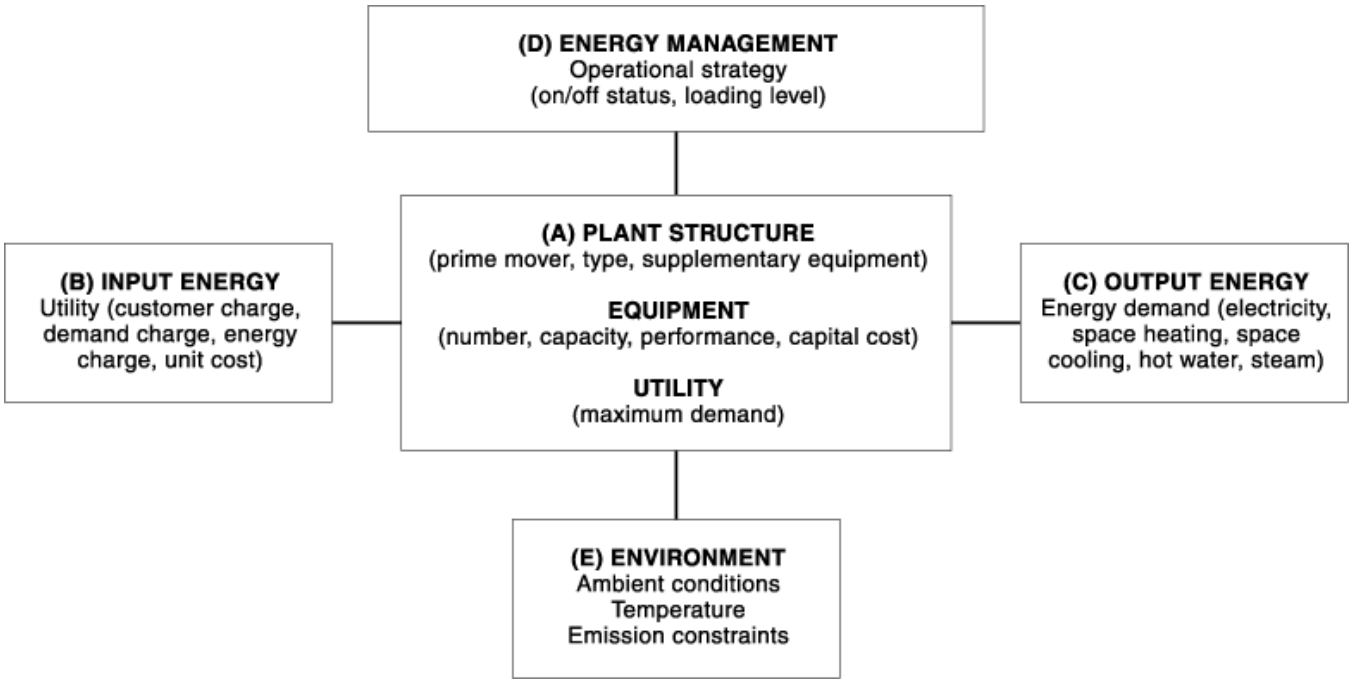


**Fig. 12.** Main factors to be taken into account in the design of cogeneration plants.

The annual running cost of each utility is the sum of the customer demand charges and energy charge. The demand charge is considered a function of the maximum utility demand, and the energy charge is calculated from the plant's operational strategy. As a constraint it is necessary to consider the performance characteristics of each piece of equipment and the energy balance relationships of each flow for average hourly energy demands estimated on several representative days in one year. In addition to the average energy demands, peak energy demands in summer and winter must be considered for equipment to supply energy during the peak periods.

Design variables consist of equipment capacities and maximum utility demands in the sizing problem (upper level) and the variables expressing the operational strategy in the operational planning problem (lower level). The two levels are interconnected by a penalty method. In this procedure, virtual energy flows are added to the existing energy flows for any plant, given at each search step, to satisfy the energy demands. For that purpose, a penalty cost is imposed on the occurrence of virtual energy flows. At the upper level, given information about the occurrence of virtual energy flows, the design variables change their values automatically to avoid the virtual energy flows, or to satisfy the energy demands. As an example, Fig. 14 shows the structure of a simple cogeneration plant (GT, BPST, ICE, fuel cells, etc., can be the prime movers).

The upper-level objective function is formulated in the following way:

$$C_{\text{total}} = C_{\text{capital}} + C_{\text{demand}} + C_{\text{energy}} \tag{6}$$

where $C_{\text{total}}$ is the annual total cost of the plant, $C_{\text{capital}}$ is the annual capital cost of the equipment, $C_{\text{demand}}$ is the customer demand charge, and $C_{\text{energy}}$ is the energy charge. $C_{\text{demand}}$ and $C_{\text{energy}}$ are both functions of the maximum demands for electricity and fuel.

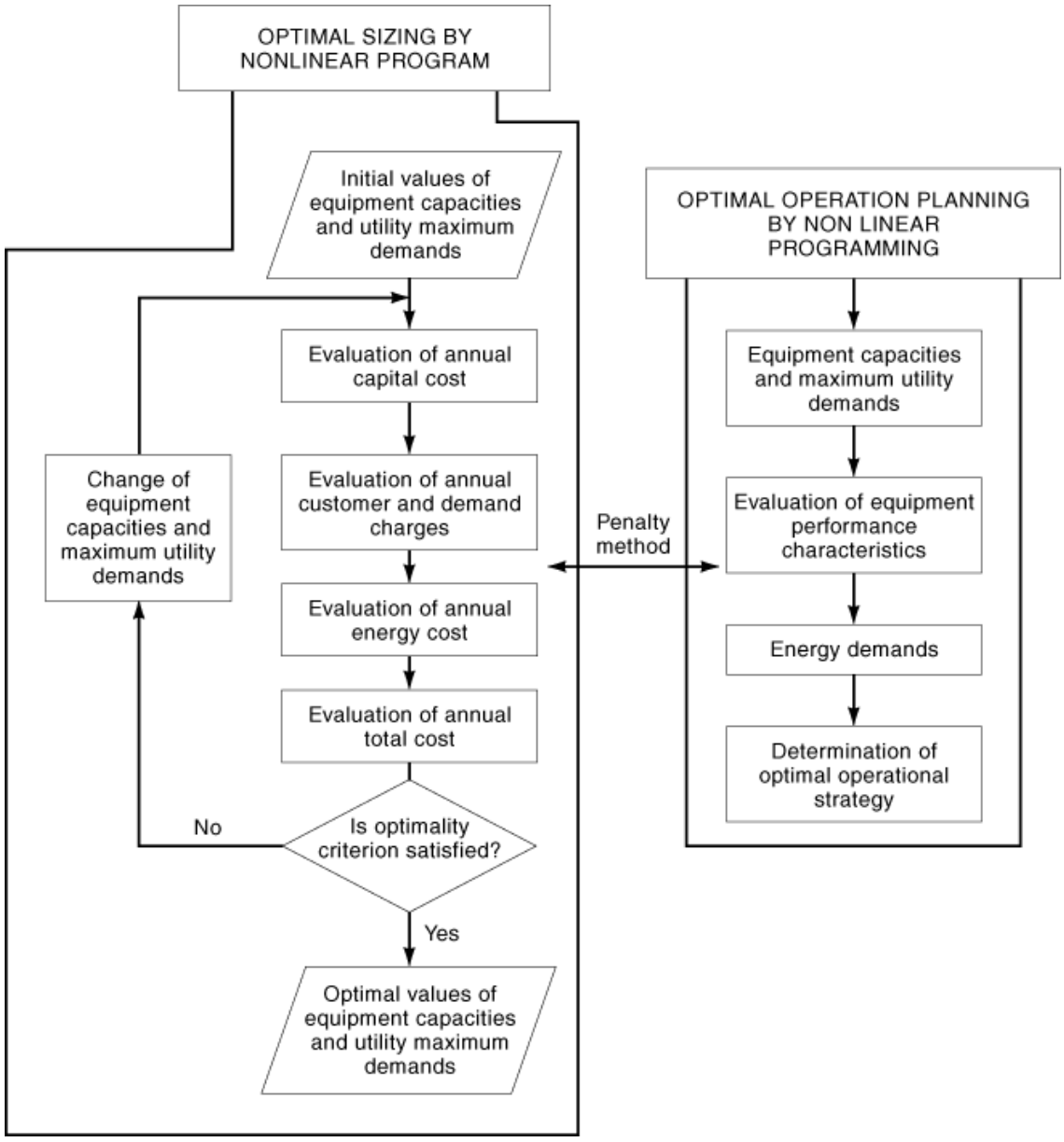


**Fig. 13.** Hierarchical algorithm for determining plants' sizes and operational strategies.

At the lower level, the objective is the minimization of the hourly energy charge for the given energy demands. The mathematical formulation of this level is very complex; it is reported by Yokohama et al. (5) for a linearized solution, and by Massardo (6) for the complete nonlinear solution.

The objective function to be minimized is expressed by

$$\varphi_{\text{buy}} E_{\text{buy}} + \varphi_{\text{fuel}} F_{\text{fuel}} + \lambda(E_{\text{pt}} + Q_{\text{pt}^c} + Q_{\text{pt}^s} + F_{\text{pt}}) \qquad (7)$$

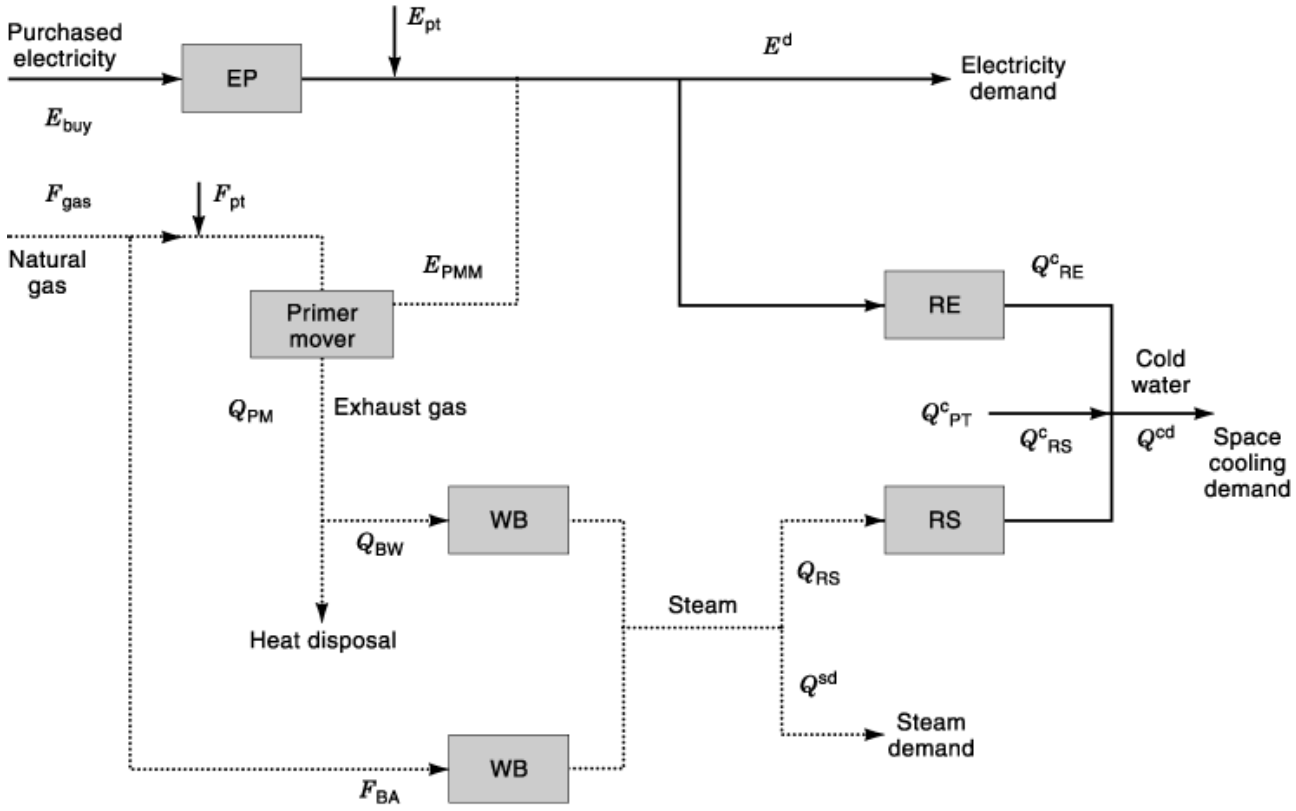


**Fig. 14.** Structure of a simple cogeneration plant.

where λ is the penalty cost, which should be given a much larger value than the utility costs $\varphi_{buy}$ and $\varphi_{fuel}$ in the numerical calculation. ($E_{pt}$, $Q_{pt}{}^c$, $Q_{pt}{}^s$, $F_{pt}$ represent virtual charges for electricity, hot water, cold water, etc. They are different than zero when the required demand is not satisfied by a plant of the size fixed at the higher level).

As an example, in Fig. 15 the load–duration curves for energy demands, indicating the annual variation of hourly demands, are presented. Hourly energy demands are given as input data for each representative day (see also Fig. 16). The functions expressing performance characteristic values and initial capital costs of equipment are determined from the actual data. In evaluating the annual capital cost, the ratio of salvage value to initial capital cost must be determined, together with the interest rate.

Several options can be investigated to obtain the optimum design and operational point of the cogeneration system. As an example, Fig. 15 shows the required and the plant duration curves (the prime mover is a phosphoric acid fuel cell), while Fig. 16 shows the heat and electricity demand for a typical day during the year (the prime mover is a diesel engine).

In this case it is possible to note that the fuel cell size is small (35 kW), compared to the maximum electrical demand (200 kW), but from the heat-demand point of view the heat-to-power ratio of the cell allows the heat–duration curve to be satisfied using a small auxiliary boiler. The small size of the cell is correlated with the high cost of the prime mover (engine) considered in the analysis (about 2500 $/kW). When a diesel engine is utilized as prime mover, its size is large (about 200 kW), and electricity is bought from the grid only during the night, when its cost is low. It is important to point out that the results for this small civil cogeneration

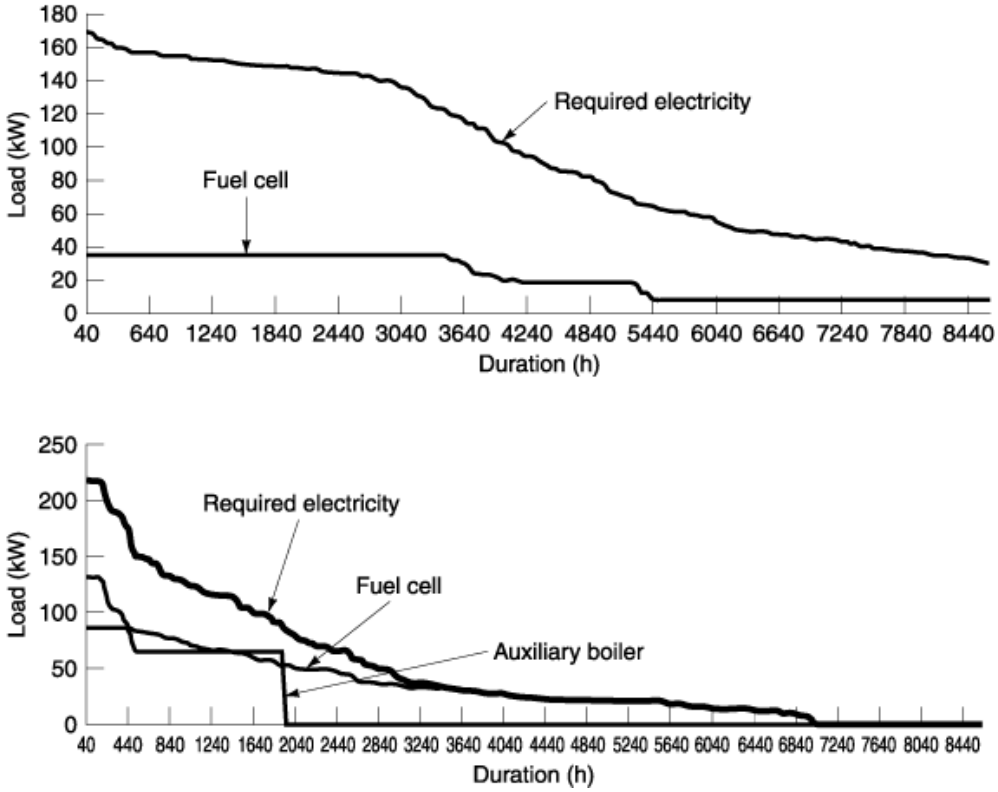


**Fig. 15.** Load–duration curves for electricity and heat supply (prime mover: phosphoric acid fuel cell).

plant have been obtained without the possibility of selling electricity to the grid. However, for large systems this option may be easily considered in the analysis.

The method is also very useful for comparisons between different plant solutions, as shown in Fig. 17, where three different solutions are compared for a civil cogeneration system (conventional layout—separated heat and electricity generation; cogeneration plant using phosphoric acid fuel cell or diesel engine). The results, reported by Massardo (6), show economic scenarios based on different fuel-cell capital costs. In this case the influence of cell cost is quite evident, and it is also interesting to note that the hierarchical optimum strategy allows one to deduce the optimum cell size from the cell cost (from 35 kW to 190 kW). The possibility of comparing different prime-mover solutions is evident in the figure, and likewise that of comparing cogeneration with conventional systems.

Another interesting approach to cogeneration plant design and management is the *thermoeconomic functional analysis* (*TFA*) proposed by Frangopoulos (7) for conventional plants and extended for modular applications by Agazzani and Massardo (8, 9). The approach is especially useful in that it yields the complete internal economy of the system based on exergy flows, which is helpful for the diagnosis of cogeneration plants. Moreover, the thermoeconomic analysis and optimization are completely nonlinear, and it is possible to take into account the environmental aspects (emissions, carbon dioxide sequestration, carbon tax, etc.) as presented by Massardo et al., (10, 11, 12).

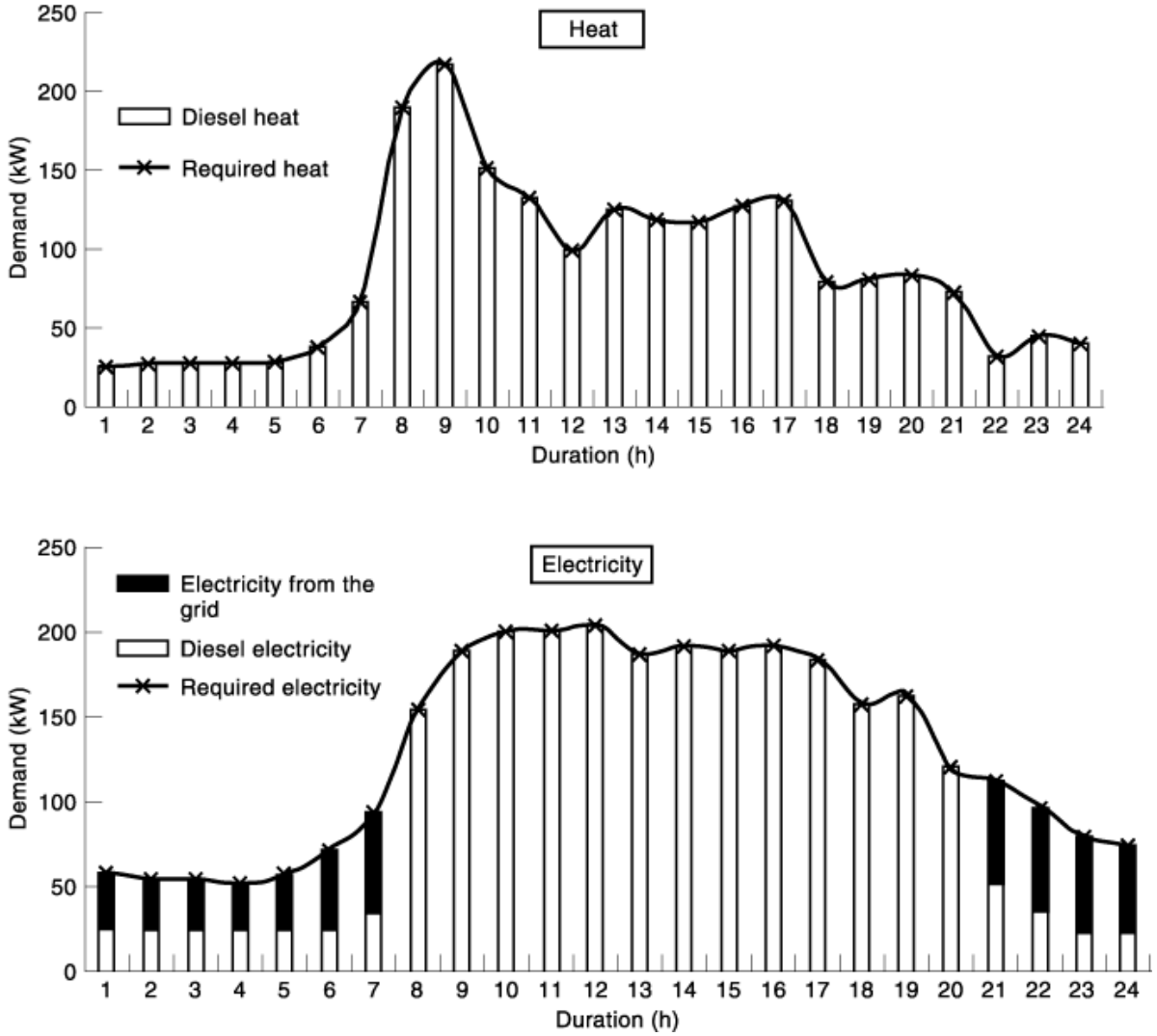


**Fig. 16.** Energy demand pattern on a representative day during the year (prime mover: diesel engine).

## Microcogeneration

During recent years, two new developments among others have aroused interest in the field of small-scale electric and heat generation, called *microcogeneration:* advanced micro gas turbines (*MGT*s) and high-temperature fuel cells [solid oxide (SOFCs) and molten carbonate (MCFCs)], as discussed by Massardo and Lubelli (13) and by Campanari and Macchi (19).

MGTs are projected to achieve net electrical efficiencies approaching 30% in the 50 kW to 300 kW range. SOFCs and MCFCs achieve 50% net electrical efficiencies for electric power production. The successful operation of a 100 kW SOFC (15) and a 100 kW MCFC (16) offers a basis for considering small plants based on the integration of these different technologies.

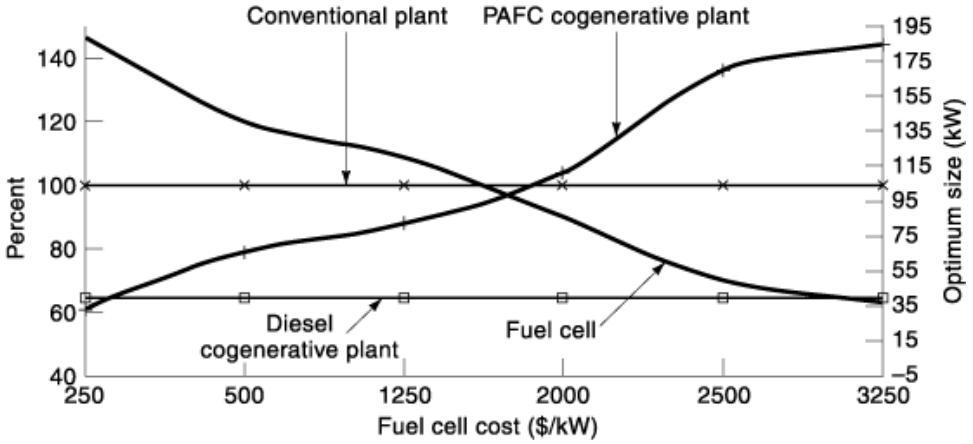


**Fig. 17.** Influence of the cost of the phosphoric acid fuel cell on the optimum size of the cogeneration system, and comparison with conventional and diesel engine cogeneration plants.

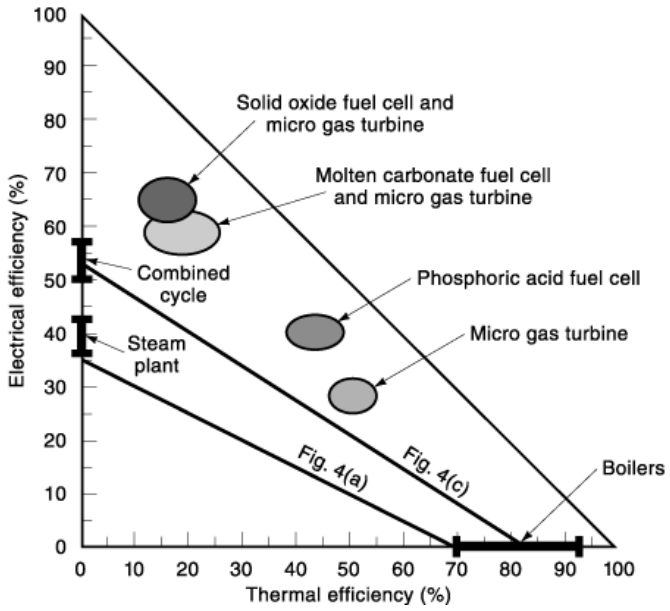


**Fig. 18.** Fuel energy saving ratio for innovative micro cogeneration systems (solid oxide fuel cell, molten carbonate fuel cell, micro gas turbine).

Figure 18 shows, as examples, the performance of the cited systems from the FESR point of view (the line for FESR = 0 from Fig. 4 is also shown). The results are noteworthy, particularly for the SOFC–MGT and MCFC–MGT systems (17): However, the cost of the cells must be carefully investigated, as discussed by Massardo (18), to be able to meet the requirements of the micro-cogeneration market, which at the moment is dominated by the ICE.

The evaluation of the energy saving achievable by the application of these novel technologies to cogeneration is an important task for the near future, particularly for civil applications, where space cooling must also be taken into account, as shown by Campanari and Macchi (19).

## BIBLIOGRAPHY


1. T. Korakianitis *et al.* Parametric performance of combined cogeneration power plants with various power and efficiency enhancements, ASME Paper 97-GT-286; *ASME Trans. J. Gas Turbines and Power* (in press).
2. R. W. Porter K. Mastanaiah Thermo-economical analysis of heat-matched industrial cogeneration systems, *Energy*, **7** (2), 171–187, 1982.
3. J. H. Horlock *Cogeneration: Combined Heat and Power*, New York: Pergamon, 1987.
4. S. Consonni G. Lozza E. Macchi Optimization of cogeneration systems operation. Part A: Prime movers modelization. Part B: Solution algorithm and example of optimum system operating strategies, presented at ASME Cogen Turbo Conf., Nice, 1989.
5. R. Yokoyama K. Ito Y. Matsumoto Optimal sizing of a gas turbine cogeneration plant in consideration of its operational strategy, *ASME J. Eng. Gas Turbines and Power*, **116**: 32–38, 1994.
6. A. F. Massardo Hierarchical fully non-linear optimal solution of the sizing and operational strategy of cogeneration systems, DIMSET-TN-15/1999, Univ. of Genoa, 1999.
7. C. A. Frangopoulos Optimal synthesis and operation of thermal system by the thermoeconomic functional approach, *ASME J. Eng. Gas Turbines and Power*, **114**: 707–714, 1992.
8. A. Agazzani A. Massardo A. Satta Thermoeconomic analysis of complex steam plants, ASME Paper 95-CTP-38; presented at ASME Cogen Turbo Power Conf., Wien, 1995.
9. A. Agazzani A. F. Massardo A tool for thermoeconomic analysis and optimization of gas, steam and combined plants, *ASME Trans. J. Eng. Gas Turbines Power*, **119**: 885–892, 1997.
10. A. Agazzani C. Frangopoulos A. Massardo Environmental influence on the thermoeconomic optimization of a combined plant with $NO_x$ abatement, *ASME Trans. J. Gas Turbines Power*, **120**: 557–565, 1998.
11. R. Borchiellini A. F. Massardo M. Santarelli Carbon tax vs. $CO_2$ sequestration effects on environomic analysis of existing power plants, presented at Conf. ECOS 1999, Tokyo, Japan; *J. Energy Resources Manage.* (in press).
12. R. Borchiellini A. F. Massardo M. Santarelli Analytical procedure for carbon tax evaluation, *Energy Conversion Manage.*, **41**: 1509–1531, 2000.
13. A. F. Massardo F. Lubelli Internal reforming solid oxide fuel cell–gas turbine combined cycles (IRSOFC–GT). Part A: Cell model and cycle thermodynamic analysis, *Trans. ASME J. Gas Turbines and Power*, **122**: 27–35, 2000.
14. S. Campanari E. Macchi Thermodynamic analysis of advanced power cycles based upon solid oxide fuel cells, gas turbines, and Rankine bottoming Cycles, ASME Paper 98-GT-585, 1998.
15. S. Veyo C. Forbes Demonstrations based on Westinghouse's prototype commercial AES design, *Proc. Third European SOFC Forum*, Nantes, 1998.
16. A. F. Massardo B. Bosio Assessment of molten carbonate fuel cell models and integration with gas and steam cycles, ASME Paper 2000-GT-174, *ASME Trans. J. Eng. Gas Turbines Power* (in press).
17. A. F. Massardo C. F. McDonald T. Korakianitis Microturbine/fuel-cell coupling for high efficiency electrical power generation, ASME Paper 2000-GT-175, *ASME Trans. J. Eng. Gas Turbines Power* (in press).
18. A. F. Massardo L. Magistri Internal reforming solid oxide fuel cell–gas turbine combined cycles (IRSOFC–GT). Part B: Exergy and thermoeconomic analysis, ASME Paper 2001-GT-0380.
19. S. Campanari E. Macchi Performance prediction of small-scale tri-generation plants based on integrated SOFC and microturbine systems, *ASME TURBOEXPO 200*, May 2000, Munich, ASME paper 2000-GT-318.


ARISTIDE F. MASSARDO
University of Genoa